International Journal for Housing Science and Its Applications

Publish September 9, 2025. Volume 47, Issue 1 Pages 801-810

https://doi.org/10.70517/ijhsa47170

Spatiotemporal Patterns and Fire Vulnerability of the Wildland–Urban Interface in China under Climate Change

Dapeng Gong[1,2,*]

[1] China Fire and Rescue Institute, Beijing 102202, China

[2] College of Forestry, Northeast Forestry University, Harbin, Heilongjiang, 150040, China

Corresponding authors: (e-mail: gdp@cfri.edu.cn).

Abstract Climate change exacerbates global wildfire risk, particularly in the wildland–urban interface (WUI), which constitutes a zone of heightened wildfire susceptibility. Understanding the spatiotemporal evolution patterns and fire vulnerability characteristics of the WUI is therefore crucial for regional ecological security and sustainable development. This study focuses on the impacts of wildfires on WUI ecosystems and human health. To assess these impacts, we developed a comprehensive fire vulnerability index. This index provides a framework for systematically evaluating the spatiotemporal evolution of China's WUI and its associated fire vulnerability patterns under various climate change scenarios. Climate change will significantly influence the future spatiotemporal evolution of China's WUI. Under the SSP1-2.6 and SSP2-4.5 scenarios, the national WUI area exhibited a significant decreasing trend, with rates of 8030 km² per decade ($p < 0.01$) and 7060 km² per decade ($p < 0.01$), respectively. By the end of the 21st century, China's WUI is projected to shift eastward. Concurrently, the boundaries between forests and urban areas are expected to become increasingly diffuse, and anthropogenic influences on surrounding forest areas will intensify. The WUI fire vulnerability is highest in southern China, particularly in Southwest (0.27--0.31), whereas northern China presents relatively lower values. Under the high-emission scenario SSP5-8.5, the national WUI fire vulnerability showed a significant increasing trend (0.00016 per year, $p < 0.01$), with particularly pronounced increases in Southwest and Northwest China. Both the spatial distribution of WUI areas and their fire vulnerability exhibit significant regional variations and scenario dependence under climate change. High-emission scenarios increase China's WUI fire vulnerability, thereby exacerbating the risk of fire-related losses across regions. This study elucidates the complex impacts of climate change on China's WUI and its fire vulnerability, providing a crucial reference for developing targeted fire prevention strategies across different regions.

Index Terms wildland–urban interface, climate change, spatial and temporal characteristics, wildfires, vulnerability

I. Introduction

The wildland–urban interface (WUI) has been an important issue in global forest fire management [1], [2]. The WUI generally has higher fuel loads than urban areas and more frequent human ignition sources than natural wildlands. This confluence of factors heightens wildfire susceptibility in the WUI, posing a serious threat to human life and property safety as well as the ecosystem [3], [4]. For example, 2025 WUI fires in Los Angeles, resulted in the destruction of approximately 16,000 structures and directly led to the evacuation of 180,000 people [5]. Wildfires that occurred during the 2019-2020 fire danger period in Australia directly resulted in 33 deaths and the destruction of 3,000 homes [6]. The promotion of China's ecological civilization and the construction of national forest cities has also contributed to the expansion of the WUI area [7], [8]. In recent years, several WUI fires have occurred in China [9], resulting in serious casualties and destruction of buildings and facilities. Furthermore, climate warming increases the frequency of high fire risk weather conditions, exacerbating WUI wildfire occurrence, magnitude, and intensity [10]. Investigating the spatiotemporal evolution of the WUI and its fire vulnerability is therefore of significant theoretical and practical importance.

The vulnerability of hazard-bearing environments is an important aspect of wildfire risk assessment [11], [12]. Vulnerability refers to the propensity of an exposed element (e.g., ecosystem, community, infrastructure) to suffer adverse effects [13]. The components of vulnerability are relatively complex, including sensitivity or susceptibility to harm and a lack of adaptive capacity, and represent the intrinsic relationship between the intensity of the causal factors causing the degree of loss of the disaster-bearing body [13], [14]. The vulnerability of natural systems is determined by regional natural resource endowment and ecological conditions, and the vulnerability of socioeconomic systems is determined by human behavior and social organization. The identification of terrestrial ecosystems and socioeconomic vulnerability is usually prioritized in disaster risk

assessment in the context of climate change [13]. Within the context of this study, WUI fire vulnerability specifically denotes the degree of expected damage or loss to exposed elements (ecosystems, human populations, infrastructure) within the WUI resulting from wildfire behavior. Whereas existing studies on WUI vulnerability have evaluated the characteristics of WUI settlements that are susceptible to fire damage [15], fire hazards are determined by identifying variables such as environmental conditions (e.g., wind speed, temperature, humidity, etc.), topography, and fuel type [16], [17], which are also used to calculate burning and ignition probabilities [18], [19]. Furthermore, fire weather conditions are strongly correlated with wildfire probability, intensity, and burned area. High fire hazard weather conditions result in low vegetation moisture content and high flammability, making fires more likely to spread and exhibit high-intensity fire behavior once they occur. [20], [21]. Accordingly, several studies have assessed the vulnerability of bearers to wildfire events in terms of fire hazard weather indices [21], [22]. Wildfires pose a serious threat to human infrastructure, ecosystem services, and residents' livelihoods in the WUI region [23], [24], and the combination of climate change and human activities exacerbates the frequency and unpredictability of wildfires [25], making strengthening wildfire management in the WUI region particularly urgent. Current fire risk assessment efforts in China predominantly focus on meteorological fire danger forecasting for large, contiguous forested or grassland areas [9]. However, quantitative assessments of fire vulnerability, particularly at the landscape scale and specifically within the WUI context, remain scarce. Under the influence of global warming, analyzing the spatial and temporal evolution of WUI regions in China in the future, and evaluating WUI fire vulnerability under climate change scenarios for different geographic regions will be helpful for scientifically responding to WUI fire risk in the context of climate change.

II. Materials and methods

II. A. Study area

The Chinese mainland was divided into six regions: Northeast (NE), North China (NC), East China (EC), South Central (SC), Northwest (NW), and Southwest (SW). This division considers both geographic location and economic development levels. The following terms are used for convenience of description: “eastern China” (including NE, NC, SC, and EC), “western China” (SW and NW), “northern China” (NE NC and NW), and “southern China” (EC, SC, and SW). The major vegetation types exhibit distinct regional distributions (Figure 1, the data used to produce this figure were obtained from https://globalmaps.github.io/). Needleleaf and broadleaf forests are distributed mainly in NE, EC, SC and eastern SW. Grasslands are located mainly in northern NC, western SW and southern NW China. Croplands are located mainly in western NE, southern NC, western EC and eastern SW.

To produce WUI maps with accurate spatial resolution for long time series, constructing a WUI identification model suitable for localized fire occurrence characteristics is crucial. In this study, we adopted the spatial zoning criterion for the WUI proposed by the FAO [26], i.e., defining the WUI in terms of "urban and wilderness buffer overlap zones", and used the buffer distance as a key element for identifying the WUI. By analyzing historical WUI fire cases in various parts of China, we quantified the buffer distance suitable for the landscape characteristics of China. The process established a buffer distance that effectively covers 90% of the WUIs. This process established a WUI buffer zone that effectively covered 90% of historical fire events [9]. On the basis of the results of this study, we mapped the spatial distribution of the WUI in China in 2020 (Figure 1). The areas with higher WUI density are mainly concentrated in economically developed and densely populated areas, especially in southeastern China.

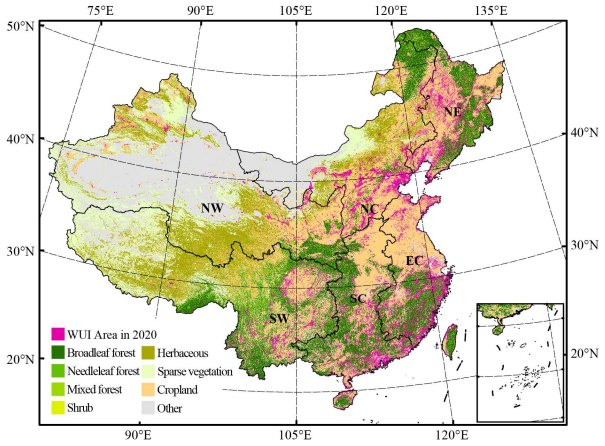

Figure 1: Study area

II. B. Data sources

(1) Fire statistics: The satellite monitoring data of forest fires from 2008--2020 came from the National Forest and Grassland Fire Prevention and Suppression Information Sharing Platform (https://slcygxpt.slcyfh.mem.gov.cn/), and the information of the satellite fire sites included the date and time of fire occurrence, longitude and latitude, the number of pixels, the continuity, the land type, and the feedback information. The satellite monitoring data were verified and checked on the ground. Forest fire statistics from the State Forestry and Grassland Administration for 1951--2020, including the number of fires, burned area, human casualties, and fire losses.

(2) Net primary productivity (NPP) data: NPP is important for characterizing plant activities and is a major factor in determining the carbon sinks of ecosystems and regulating ecological processes. We utilized the MODIS product (MOD17A3HGF.061) to generate a China NPP dataset for 2001--2023. This dataset has a spatial resolution of 500 m and was mosaicked to cover the study area.

(3) Land use/land cover data: Future WUI regions were delineated using projected land use/land cover data from Luo et al. [27]. This dataset provides 1-km resolution gridded projections for China under 24 combined SSP-RCP scenarios, spanning the period 2020--2100. It models future LULC changes on the basis of shared socioeconomic pathways (SSPs) and representative concentration pathways (RCPs).

(4) Meteorological data: Meteorological data were obtained from surface observations of the China Meteorological Administration, including daily maximum temperature, minimum relative humidity, average wind speed and daily precipitation, and were screened according to the missing proportion of elements (not higher than 5%) during the study period at each site. The outliers and missing values were corrected for the remaining 2,207 valid sites after the screening process and interpolated using multiple linear regression analyses [28]. The model information uses historical climate simulation test data from the CMIP6 climate model with future scenario test data (https://esgf-node.llnl.gov/search/cmip6/). CMIP6 incorporates diverse shared socioeconomic pathways (SSPs), representing the latest anthropogenic emission trajectories and potential future societal development pathways, including efforts related to climate change mitigation and adaptation [29].Given the large number of CMIP6 models, we selected four models (CanESM5, CMCC-CM2-SR5, EC-Earth3, and EC-Earth3-Veg-LR) known for their relatively high performance over China and possessing more complete data availability for both historical and future scenarios [30], [31]. Owing to the uncertainties in the parameterization and structure of the existing models, each model behaves differently in different regions of the globe [32]. To reduce model simulation uncertainty, a weighted multi-model ensemble (MME) [33] mean was calculated for each scenario. We selected three SSP-RCP scenarios: SSP1-RCP2.6 (representing sustainable development), SSP2-RCP4.5 (moderate development), and SSP5-RCP8.5 (conventional development). The historical period 1985--2014 served as the baseline, whereas the end-of-century period 2071--2100 was used to assess future spatial changes in WUI fire vulnerability.

II. C. Statistical analysis

(1) Trend analysis: In the characterization of the WUI and vulnerability evolution, a simple linear regression model is used for regression analysis, and the calculation formula is as follows:

$$\theta = \frac{n \times \sum_{i=1}^{n} (i \times C_i) - \sum_{i=1}^{i} i \sum_{i=1}^{i} C_i}{n \times \sum_{i=1}^{n} i^2 - (\sum_{i=1}^{i} i)^2} \tag{1}$$

where θ is the slope of the trend of feature C over a multiyear time series, n is the number of years in the time series, and C_i is the value of C *in the ith* year.

(2) Dynamic rate: The dynamic rate of land use is mainly used to measure the future trend of land use [34], and here we use it to measure the dynamic rate of a single WUI region in different areas. The formula is as follows:

$$K = \frac{(U_b - U_a)}{U_a} \times \left(\frac{1}{T}\right) \times 100\% \tag{2}$$

where T represents the study period (year); K represents the dynamic rate of the WUI area during the study period; U_a represents the land area of the WUI area at the beginning of the study period; and U_b represents the land area of the WUI area at the end of the study period.

II. D. Vulnerability assessment

Within the operational context of this vulnerability assessment framework, we quantify WUI fire vulnerability as the degree of expected damage or loss to exposed elements (ecosystems and human populations) resulting from wildfire behavior, reflecting both their inherent susceptibility and the prevailing conditions influencing loss magnitude. In accordance with the

results of previous studies, this study used the decrease in net primary productivity (NPP) of vegetation during wildfires in the WUI region to characterize the effects of wildfires on ecosystems [35], [36], used the casualties caused by wildfires in WUI regions to characterize the impacts on the health of urban residents [21], [37], and established a functional relationship between the fire weather index (FWI) and damage during fires [36], [37]. The fire hazard weather index is calculated on the basis of historical observations and data from future climate scenarios [38]. Min–max normalization was performed for the raw data to eliminate the differences in the distribution and magnitude of the data. This study evaluated the vulnerability of the WUI to wildfire events in terms of both terrestrial ecosystems and social activities. The standardized scores for NPP loss and human casualties (denoted as SC_i^{NPP} and SC_i^{Cas}) are summed to calculate the vulnerability index (v_i) for each assessment unit i:

$$v_i = SC_i^{\mathrm{NPP}} + SC_i^{\mathrm{Cas}} \tag{3}$$

where v_i denotes the vulnerability index of the bearer in the ith assessment unit to a WUI fire event and where SC_i^{NPP} and SC_i^{Cas} are the NPP loss and human casualties in the corresponding WUI area, respectively. A high v_i value represents a high vulnerability of the bearer to a WUI fire event. The Jenks break method was also used to classify WUI fire vulnerability.

III. Results

III. A. Characteristics of WUI evolution

III. A. 1) Future temporal characteristics of the WUI

Temporally, the national WUI area exhibited a decreasing trend across all future scenarios (Figure 2). Specifically, under the SSP1–2.6 and SSP2–4.5 scenarios, the decreasing trends were statistically significant ($p < 0.01$), with rates of 8030 km^2 per decade and 7060 km^2 per decade, respectively, and there was no significant trend of change in the WUI under the SSP5–6.0 scenario ($p = 0.466$), which generally showed a trend of decreasing and then increasing. The trend of each region under the different scenarios was basically consistent with that of the whole country (Table 1), and the WUI area of each region under the SSP1–2.6 and SSP2–4.5 scenarios exhibited a significant decreasing trend ($p < 0.01$, except for NE under the SSP2–4.5 scenario), among which the SC exhibited the fastest decreasing trend, with different scenarios of −0.229 and −0.215 × 10^{4}km^2/10a; there was no significant trend ($p > 0.05$) in the WUI area of each region under the SSP5–6.0 scenario.

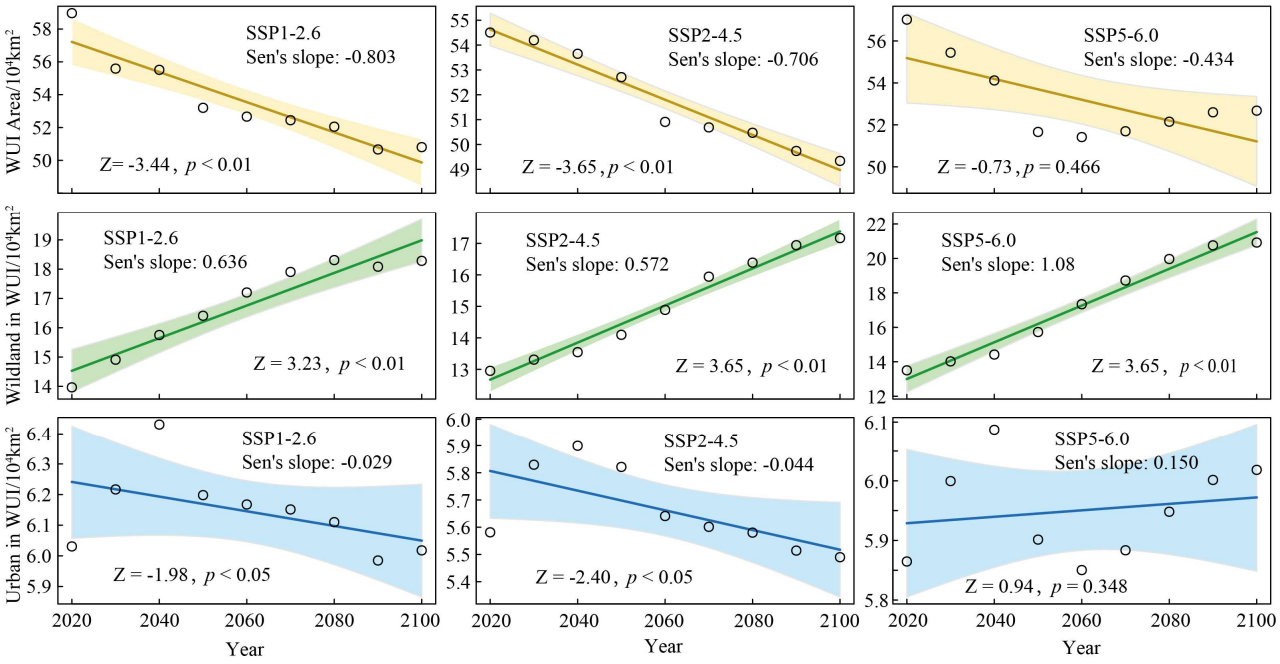

Figure 2: Trend evolution of China's WUI region under different scenarios

To analyze the characteristics of WUI changes more deeply, we extracted the areas of towns and forests within the WUI, in which the areas of forests in the WUI regions presented a significant increasing trend ($p < 0.01$), and the rates of increase in forest areas in the WUI under different climate change scenarios were, in descending order, SSP5–6.0 (1.08 × 10^{4}km^2/10a), SSP1–2.6 (0.636 × 10^{4}km^2/10a) and SSP2–4.5 (0.572 × 10^{4}km^2/10a), whereas the areas of towns and cities built in the WUI region (anthropogenic area) varied in the trend of change in different scenarios, with the overall trend of towns and cities in the WUI in the SSP1–2.6 and SSP2–4.5 scenarios showing a decreasing trend ($p < 0.05$), and there was no obvious trend of

change under the SSP5–6.0 context (p = 0.348), basically maintaining a more stable area range. This trend is consistent with the results of Luo et al. [27], i.e., China's cities and towns continue to grow rapidly before 2040 and basically remain stable after 2040.

Table 1: Trends in the evolution of the WUI in different scenarios by region

Region	Parameter	Scenario		
		SSP1–2.6	SSP2–4.5	SSP5–6.0
Mainland China	Sen's slope	–0.803	–0.706	–0.434
	Z	–3.44	–3.65	–0.73
	p	<0.01	<0.01	0.466
East China	Sen's slope	–0.135	–0.149	–0.057
	Z	–2.19	–2.81	–0.73
	p	<0.05	<0.01	0.466
North China	Sen's slope	–0.149	–0.201	0.012
	Z	–3.44	–3.65	1.36
	p	<0.01	<0.01	0.175
Northeast	Sen's slope	–0.110	0.078	–0.006
	Z	–3.02	1.36	–0.10
	p	<0.01	0.175	0.917
Northwest	Sen's slope	–0.025	–0.047	0.002
	Z	–3.65	–3.44	0.73
	p	<0.01	<0.01	0.466
South Central	Sen's slope	–0.229	–0.215	–0.183
	Z	–3.44	–3.23	–1.56
	p	<0.01	<0.01	0.118
Southwest	Sen's slope	–0.173	–0.180	–0.170
	Z	–3.44	–3.44	–1.56
	p	<0.01	<0.01	0.118

III. A. 2) Future spatial characteristics of the WUI

On a spatial scale, the evolution of different regions under different scenarios is basically the same. Figure 3 depicts the spatial distribution of changes in the WUI across China between the early (2020) and late (2100) 21st centuries under three climate change scenarios: SSP1–2.6, SSP2–4.5, and SSP5–6.0. The figure 3 shows that by the end of the 21st century, the areas of increasing WUI in China are concentrated mainly on the southeastern coast of China (economically developed and highly populated areas) and the NE (extensive forest vegetation cover), whereas the areas of decreasing WUI are concentrated mainly in the central part of China (including the eastern part of SW, the northern part of SC, and the western part of EC), as well as in parts of the NE. The locations of spatial changes under the three climate change scenarios are basically the same, which indicates that the overall pattern of future spatial changes in the WUI is relatively insensitive to the selected emission scenarios.

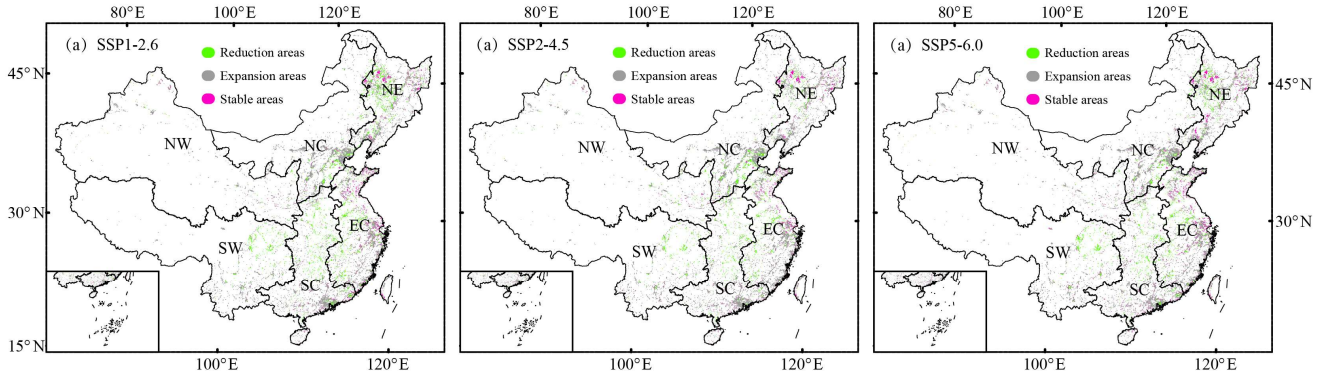

Figure 3: Spatial changes in the WUI across China under three climate change scenarios (SSP1–2.6, SSP2–4.5, and SSP5–6.0) from 2020––2100

In terms of the differences among regions, the ranking of the WUI area in each region under different future climate change scenarios did not change, and the order was EC, NE, SC, NC, SW, and NW (Table 2). By the end of the 21st century (2100), the national WUI land use dynamic rates under the three climate change scenarios (SSP1–2.6, SSP2–4.5, and SSP5–6.0) will be –1.54%, –1.05, and –0.85%, respectively, which show a decreasing dynamic trend, and the dynamic rate will be even lower under high social forcing and high radiative forcing, which is consistent with the results of the time trend analysis. The dynamic rates under different scenarios in EC and SC are consistent with the national trend and are the main WUI area increasing regions in China, while the dynamic rates under different scenarios in SW are lower than those in other regions, and this decreasing trend is mainly concentrated in the northeast part of SW (Sichuan and Chongqing Provinces). The WUI area in NW is always much lower than that in other regions, the future WUI land use changes under different climatic scenarios are small, the absolute value of the dynamic rates is the lowest and close to 0, and its special geographic and climatic environment is analyzed.

Table 2: WUI area and dynamic rate in different scenarios by region

Region	WUI area (10^4 km^2) in 2020			WUI area (10^4 km^2) in 2100			Dynamic rate/%		
	SSP1–2.6	SSP2–4.5	SSP5–6.0	SSP1–2.6	SSP2–4.5	SSP5–6.0	SSP1–2.6	SSP2–4.5	SSP5–6.0
Mainland China	58.97	54.51	57.02	50.81	49.34	52.68	–1.54%	–1.05%	–0.85%
East China	14.06	13.61	13.99	13.01	12.69	13.56	–0.83%	–0.75%	–0.34%
North China	10.66	10.48	10.43	9.37	8.93	9.69	–1.34%	–1.64%	–0.79%
Northeast	12.39	10.00	11.08	10.33	10.26	10.57	–1.85%	0.29%	–0.51%
Northwest	3.97	4.03	3.93	3.76	3.65	3.91	–0.59%	–1.05%	–0.06%
South Central	11.74	10.93	11.40	9.66	9.50	10.08	–1.97%	–1.45%	–1.29%
Southwest	6.15	5.46	6.19	4.67	4.31	4.87	–2.67%	–2.34%	–2.37%

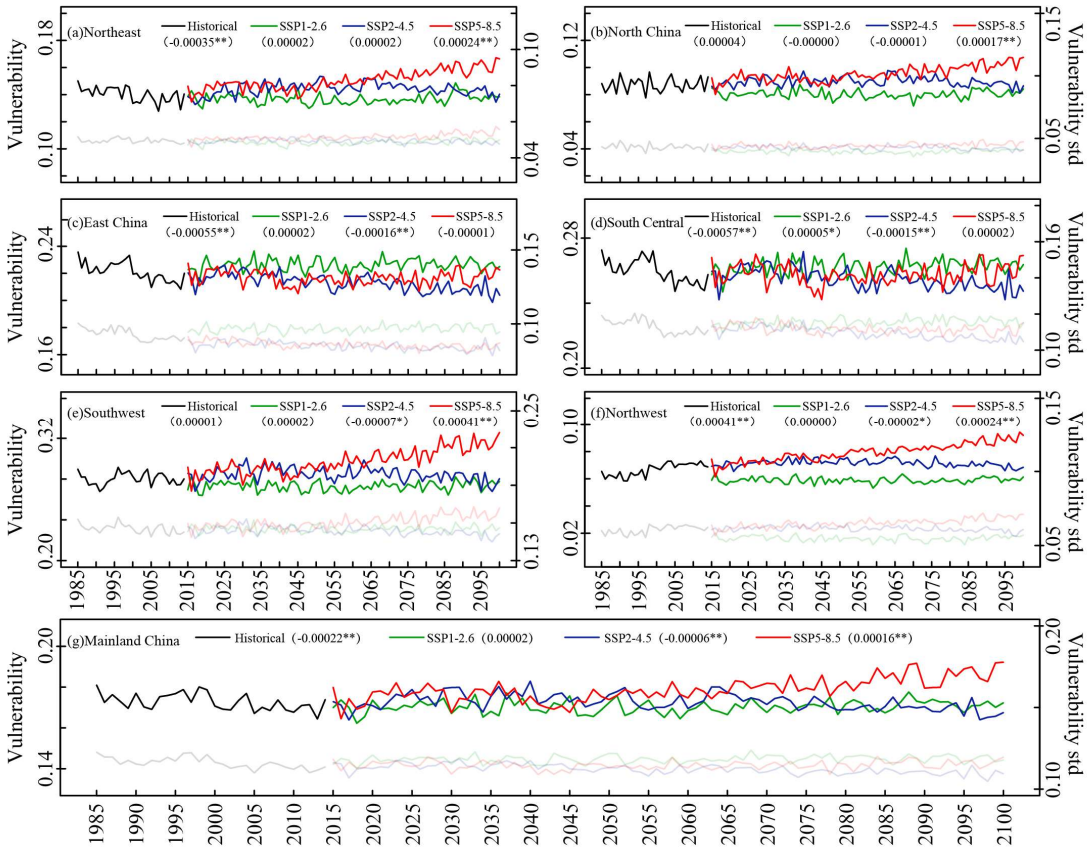

Figure 4: Temporal trends in the vulnerability of WUI regions in China under different climate scenarios

Note: The numbers in parentheses in the legend represent the rate of linear change over time; *$p < 0.05$, **$p < 0.01$.

III. B. Vulnerability assessment of WUI fires

III. B. 1) Future temporal characteristics of WUI fire vulnerability

Temporally, the national WUI fire vulnerability exhibited divergent trends under different climate change scenarios (Figure 4). During the historical baseline period (1985−−2014), national WUI fire vulnerability showed a significant decreasing trend ($p < 0.01$), with a rate of −0.00022 per year. Future trends in China's WUI fire vulnerability diverge markedly across climate change scenarios, and China's WUI fire vulnerability under the SSP1−2.6 (sustainable development) scenario remains within a stable range, with no significant change trend ($p > 0.05$), indicating that WUI fire vulnerability under this sustainable development pathway remains stable at a relatively lower level. Under the SSP2−4.5 (moderate development) scenario, China's WUI fire vulnerability shows a lower rate of decrease (−0.00006/a, $p < 0.01$), which is less different from the range of WUI fire vulnerability under the SSP1−2.6 scenario, whereas under the SSP5−8.5 (conventional development) scenario, the national WUI fire vulnerability shows a significant and rapidly increasing trend (0.00016/a, $p < 0.01$).

From the time−varying trend of each region, there is a divergence in the trend of WUI fire vulnerability under different climate change scenarios. In the historical base period, the WUI fire vulnerability in NE, EC, and SC presented the same evolutionary characteristics as the whole country did, with a significant decreasing trend ($p < 0.01$) and decreasing rates of 0.00035/a, 0.00055/a, and 0.00041/a, respectively, whereas NC and SW presented stable trends, and only NW WUI fire vulnerability exhibited a significant increasing trend ($p < 0.01$), with a growth rate of 0.00041/a. Under the SSP1−2.6 scenario, only SC shows a significant growth trend ($p < 0.05$), and the WUI fire vulnerability of all other regions remains stable and does not show a significant trend of change. Under the SSP2−4.5 scenario, there is no significant trend of change in NE and NC, and all other regions show a significant decreasing trend ($p < 0.05$), of which EC and SC have larger decreasing rates of 0.00016/a and 0.00015/a, respectively. Under the SSP5−8.5 scenario, there is no significant trend of change in SC and NC, and other regions show a significant increasing trend ($p < 0.01$). Overall, WUI fire vulnerability in southeastern China (EC and SC) will remain stable or decrease under future scenarios, which will be conducive to coping with the risks posed by WUI fires. However, the WUI fire vulnerability in NE and NC will remain stable or increase, which will increase the risks posed by WUI fires. SW and NW showed very different trends under the three climate change scenarios, i.e., SSP1−2.6 remained stable, SSP2−4.5 decreased significantly, and SSP5−8.5 increased very significantly, which needs to be further investigated to reveal the underlying reasons.

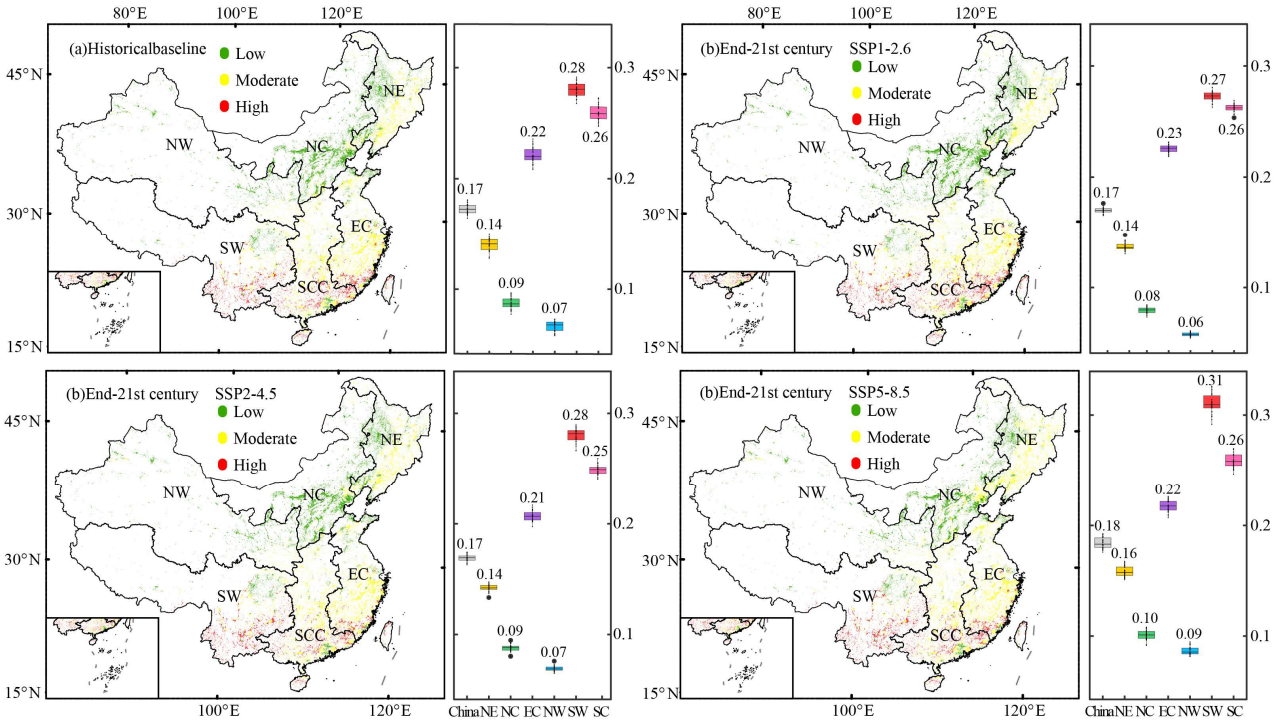

Figure 5: presents the spatial distribution (grid map) and regional statistics (box plot) of WUI fire vulnerability levels under different climate scenarios

III. B. 2) Future spatial characteristics of WUI fire vulnerability

Spatially, the distribution patterns of WUI fire vulnerability were broadly consistent across the three climate change scenarios during both the historical baseline (1985−−2014) and the end of the 21st century (2071−−2100) periods (Figure 5). Regions exhibiting high WUI fire vulnerability, both historically and in future projections, are predominantly located in southern China. SW consistently presented the highest average vulnerability (0.27−−0.31), followed by SC (0.25−−0.26) and EC (0.21−−0.23). The vulnerability in these three southern regions exceeded the national average (0.17−−0.18). Although SW has the highest average vulnerability, the high-vulnerability regions are mainly concentrated in Yunnan and Guizhou Provinces. Other regions of high vulnerability in China are concentrated in the southern part of the SC (Guangxi and Guangdong Provinces) and in the southern part of the EC (Fujian Province). Areas of moderate vulnerability are located mainly in central China and parts of NE China. In addition, no high vulnerability areas were observed in the northern regions of China (NW, NC, and NE) under the different climate change scenarios. The WUI fire vulnerability is the lowest in NW, at 0.06−−0.09, followed by NC (0.08−−0.10) and NE (0.14−−0.16), which are lower than the national average WUI fire vulnerability level.

IV. Discussion

This study focuses on the spatial and temporal evolution of the WUI and its fire vulnerability in China. By integrating multisource data and CMIP6 scenario simulations, this study provides a national-scale quantification of the trend of WUI area change and spatial eastward movement under different emission pathways and constructs a two-dimensional vulnerability assessment model that integrates ecosystem productivity loss and human casualties. In this study, we found that WUI evolution and vulnerability are characterized by both regional heterogeneity and scenario dependence. In contrast to the global trend of WUI expansion [2], China's WUI area contracts significantly under low-emission scenarios. This contraction may stem from more efficient land resource utilization driven by urbanization intensification (e.g., compact city policies) and a consequent reduction in sprawl within urban–rural transition zones. The increase in forest area in the WUI (SSP5-6.0 up to 1.08×10^4 km^2/10a) reflects the positive effect of ecological engineering, but simultaneously leads to blurring of the "fuel-urban" boundary and the creation of novel zones of integrated fire risk. Furthermore, the spatial distribution of the WUI in China has undergone an eastward shift, aligning with the trajectory of China's economic center of gravity and major population movements [39]. The expansion of the WUI along the southeast coast is due to the spread of urban agglomerations (e.g., the Yangtze River Delta and the Pearl River Delta), while the increase in NE is associated with abundant forest resources but weak fire prevention infrastructure in towns and cities. The significant contraction of the WUI in the southwest region (dynamic rate: −2.67%) may be linked to sustained policies such as the Grain-for-Green program. However, this reduction warrants caution, as the decline in human activity can lead to increased fuel continuity in these areas, potentially increasing the risk of high-intensity wildfires.

In recent years, under the guidance of active fire prevention and suppression policies, the number and area of wildfires (including WUI fires) in China have significantly decreased, and the resulting ecological losses and human casualties have also shown a decreasing trend [21]. Consequently, the significant declining trend in WUI fire vulnerability observed during the historical baseline period aligns with documented improvements in China's historical WUI fire situation [9]. In contrast, under the SSP5-8.5 (conventional development) scenario, the national WUI fire vulnerability showed a significant and rapid increasing trend (0.00016/a, $p < 0.01$), which was directly associated with the amplifying effect of climate change on fire weather [40]. The decrease in vulnerability during the historical period was due to improvements in China's forest fire prevention system, but future high-emission scenarios may exceed the carrying capacity of the current prevention system. The primary concentration of high WUI fire vulnerability occurs in southern China. Southern high-vulnerability regions encompass forest ecosystems characterized by high biomass and carbon density (e.g., subtropical broadleaf evergreen forests in Yunnan and Guizhou Provinces), and the absolute and relative ecological impacts of fire-induced NPP loss are considerable, whereas northwestern grassland and northern China farmland ecosystems have low baseline values of NPP, and the recovery of herbaceous vegetation after fires is relatively fast [41], weakening the absolute magnitude of NPP loss; at the same time, the high population density, complex urban–rural intersection zones, and frequent human activities in these regions increase the probability of fire sources, and the topography (e.g., southwestern mountainous areas) and community evacuation conditions significantly increase the threat of wildfires to people's safety [9], resulting in a high risk of human casualties. This spatial coupling of high NPP loss potential with high social exposure (population, property) is the main cause of much greater vulnerability in southern China than in northern China.

Owing to data availability limitations, the WUI fire vulnerability assessment in this study did not quantify infrastructure fire resilience (e.g., fire barrier density), which may underestimate the adaptation potential in economically developed regions; furthermore, the fire weather index did not consider anthropogenic fire dynamics, and the risk in the anthropogenic areas of the southeastern coastal region, in particular, may have been underestimated. Future research needs to introduce resilience parameters (e.g., the building fire protection level) and incorporate residents' risk perceptions and emergency response capacity into the vulnerability assessment system.

V. Conclusion

Accelerating urbanization coupled with intensifying climate change has positioned the WUI as a focal area for concentrated wildfire risk, posing significant threats to life, property, and regional socioeconomic development. This study analyzes the spatial and temporal evolution characteristics of WUI areas in China and evaluates the vulnerability of WUI fires to climate change scenarios in different geographic regions. Our results demonstrate that the spatial and temporal distributions and evolution characteristics of the WUI in China are projected to be significantly influenced by climate change in the future. Under the low emission scenario (SSP1–2.6), the national WUI area is projected to decrease, the forest area in the WUI increases, the built-up area of cities and towns decreases, the boundary between forests and cities and towns tends to be blurred, and the radiative impacts of human activities on forests increase. The regional analysis revealed that the WUI area in SC decreased most significantly, whereas the southeastern coast and NE emerged as the primary areas of WUI area growth, and the spatial distribution of the WUI showed an eastward trend. Although the impacts of different climate change scenarios on the evolution of WUI landscape characteristics are not obvious, the spatial distribution and evolution of the WUI are still closely related to the future economic development and intensity of human activities in China, especially in EC, NE, and SC, which will become the main distribution areas of the WUI.

The high WUI fire vulnerability region is concentrated mainly in southern China, especially in SW, while that in northern China is relatively low. China's WUI fire vulnerability exhibited a decreasing trend during the historical baseline period, while the trend of WUI fire vulnerability under future climate change scenarios revealed significant geographic and scenario differences. The high-emission scenario (SSP5–8.5) markedly increases national vulnerability, highlighting the urgent need for adaptive strategies in SW and NW. This study reveals the complex impacts of climate change on WUI fire vulnerability in China and provides an important reference for the development of targeted fire prevention and control strategies in the future.

Data Sharing Agreement

The datasets used and/or analyzed during the current study are available from the corresponding author on reasonable request.

Competing Interests

The authors have no relevant financial or non-financial interests to disclose.

Acknowledgment

This study was supported by the China Fire and Rescue Institute Scientific Research Project [XFKZD202502; 2025RGZN04] and the Key Technologies for Preventing Safety Risks in the Construction and Operation of Photovoltaic Projects.

References

[1] MODUGNO S, BALZTER H, COLE B, et al. Mapping regional patterns of large forest fires in Wildland–Urban Interface areas in Europe. Journal of Environmental Management, 2016, 172: 112-126.https://doi.org/10.1016/j.jenvman.2016.02.013

[2] SCHUG F, BAR-MASSADA A, CARLSON A R, et al. The global wildland–urban interface. Nature, 2023, 621(7977): 94-99. https://doi.org/10.1038/s41586-023-06320-0

[3] BALCH J K, BRADLEY B A, ABATZOGLOU J T, et al. Human-started wildfires expand the fire niche across the United States. Proceedings of the National Academy of Sciences, 2017, 114(11): 2946-2951. https://doi.org/10.1073/pnas.1617394114

[4] MIRANDA A, CARRASCO J, GONZáLEZ M, et al. Evidence-based mapping of the wildland-urban interface to better identify human communities threatened by wildfires. Environmental Research Letters, 2020, 15(9): 094069. https://doi.org/10.1088/1748-9326/ab9be5

[5] QIU M, CHEN D, KELP M, et al. The rising threats of wildland-urban interface fires in the era of climate change: The Los Angeles 2025 fires. The Innovation, 2025, 6(5): 100835.https://doi.org/10.1016/j.xinn.2025.100835

[6] FILKOV A I, NGO T, MATTHEWS S, et al. Impact of Australia's catastrophic 2019/20 bushfire season on communities and environment. Retrospective analysis and current trends. Journal of Safety Science and Resilience, 2020, 1(1): 44-56.https://doi.org/10.1016/j.jnlssr.2020.06.009

[7] ZHANG Y, ZHANG T, ZENG Y, et al. Designating National Forest Cities in China: Does the policy improve the urban living environment?. Forest Policy and Economics, 2021, 125: 102400.https://doi.org/10.1016/j.forpol.2021.102400

[8] CHEN R, LI X, HU Y, et al. Road Extraction From Remote Sensing Images in Wildland–Urban Interface Areas. IEEE Geoscience and Remote Sensing Letters, 2022, 19: 1-5. https://doi.org/10.1109/lgrs.2020.3028468

[9] GONG D, SUN L, HU T. Characterizing the occurrence of wildland-urban interface fires and their important factors in China. Ecological Indicators, 2024, 165: 112179.https://doi.org/10.1016/j.ecolind.2024.112179

[10] WU Z, HE H S, KEANE R E, et al. Current and future patterns of forest fire occurrence in China. International Journal of Wildland Fire, 2020, 29(2): 104-119. https://doi.org/10.1071/WF19039

[11] SCOTT J H, THOMPSON M P, CALKIN D E. A Wildfire Risk Assessment Framework for Land and Resource Management. USDA Forest Service - General Technical Report RMRS-GTR, 2013, (315): 1-83.

[12] JOHNSTON L M, WANG X, ERNI S, et al. Wildland fire risk research in Canada. Environmental Reviews, 2020, 28: 164-186. https://doi.org/10.1139/er-2019-0046

[13] PARRY M A J, CANZIANI O, STRIHOU J-P V Y D, et al. Climate Change 2007: Impacts, Adaptation and Vulnerability. Contribution of Working Group II to the Fourth Assessment Report of the Intergovernmental Panel on Climate Change, F, 2007. https://doi.org/10.2134/jeq2008.0015br

[14] PASTOR E, CABALLERO D, RODRíGUEZ I, et al. Vulnerability analysis to wildland-urban interface fires in metropolitan areas: an integrated approach. Accés obert: Comunicació de congrés, 2022.https://doi.org/10.14195/978-989-26-2298-9_123
[15] REDUCTION U N I S F D. 2009 UNISDR terminology on disaster risk reduction. Geneva; UNISDR. 2009. https://www.undp.org/sites/g/files/zskgke326/files/migration/ge/GE_isdr_terminology_2009_eng.pdf
[16] HYSA A. Indexing the vegetated surfaces within WUI by their wildfire ignition and spreading capacity, a comparative case from developing metropolitan areas. International Journal of Disaster Risk Reduction, 2021, 63: 102434.https://doi.org/10.1016/j.ijdrr.2021.102434
[17] GHERMANDI L, BELETZKY N A, DE TORRES CURTH M I, et al. From leaves to landscape: A multiscale approach to assess fire hazard in wildland-urban interface areas. Journal of Environmental Management, 2016, 183: 925-937.https://doi.org/10.1016/j.jenvman.2016.09.051
[18] ALCASENA F J, SALIS M, AGER A A, et al. Assessing Wildland Fire Risk Transmission to Communities in Northern Spain. Forests, 2017, 8(2): 30. https://doi.org/10.3390/f8020030.
[19] ARGAñARAZ J P, RADELOFF V C, BAR-MASSADA A, et al. Assessing wildfire exposure in the Wildland-Urban Interface area of the mountains of central Argentina. Journal of Environmental Management, 2017, 196: 499-510.https://doi.org/10.1016/j.jenvman.2017.03.058
[20] TIAN X, MCRAE D, JIN J-Z, et al. Wildfires and the Canadian Forest Fire Weather Index system for the Daxing'anling region of China. International Journal of Wildland Fire, 2012, 20: 963-973. https://doi.org/10.1071/WF09120
[21] ZONG X, TIAN X, YAO Q, et al. An analysis of fatalities from forest fires in China, 1951–2018. International Journal of Wildland Fire, 2022, 31(5): 507-517. https://doi.org/10.1071/wf21137
[22] ZONG X, TIAN X, FANG L. Assessing wildfire risk and mitigation strategies in Qipanshan, China. International Journal of Disaster Risk Reduction, 2022, 80: 103237.https://doi.org/10.1016/j.ijdrr.2022.103237
[23] BURKE M, DRISCOLL A, HEFT-NEAL S, et al. The changing risk and burden of wildfire in the United States. Proceedings of the National Academy of Sciences, 2021, 118: e2011048118.https://doi.org/10.1073/pnas.2011048118
[24] PETTINARI M L, CHUVIECO E. Fire Danger Observed from Space. Surveys in Geophysics, 2020, 41(6): 1437-1459.https://doi.org/10.1007/s10712-020-09610-8
[25] PAUSAS J G, KEELEY J E. Wildfires and global change. Frontiers in Ecology and the Environment, 2021, 19(7): 387-395.https://doi.org/10.1002/fee.2359
[26] FAO. Guidelines on Fire Management in Temperate and Boreal Forests. 2002.https://www.fao.org/4/ag041e/AG041E00.htm
[27] LUO M, HU G, CHEN G, et al. 1 km land use/land cover change of China under comprehensive socioeconomic and climate scenarios for 2020–2100. Scientific Data, 2022, 9(1): 110. https://doi.org/10.1038/s41597-022-01204-w
[28] TSINKO Y, BAKHSHAII A, JOHNSON E A, et al. Comparisons of fire weather indices using Canadian raw and homogenized weather data. Agricultural and Forest Meteorology, 2018, 262: 110-119.https://doi.org/10.1016/j.agrformet.2018.07.005
[29] O'NEILL B C, TEBALDI C, VUUREN D P V, et al. The Scenario Model Intercomparison Project (ScenarioMIP) for CMIP6. Geoscientific Model Development, 2016, 9: 3461-3482.https://doi.org/10.5194/gmd-9-3461-2016
[30] SU B, HUANG J, MONDAL S K, et al. Insight from CMIP6 SSP-RCP scenarios for future drought characteristics in China. Atmospheric Research, 2020, 250: 105375.https://doi.org/10.1016/j.atmosres.2020.105375
[31] YOU Q, CAI Z, WU F, et al. Temperature dataset of CMIP6 models over China: evaluation, trend and uncertainty. Climate Dynamics, 2021, 57(1): 17-35.https://doi.org/10.1007/s00382-021-05691-2
[32] ZHU Z, ZHU Z, PIAO S, et al. Greening of the Earth and its drivers. Nature Climate Change, 2016, 6: 791-795.https://doi.org/10.1038/nclimate3004
[33] XU C, MCDOWELL N G, FISHER R A, et al. Increasing impacts of extreme droughts on vegetation productivity under climate change. Nature Climate Change, 2019, 9: 948 – 953.https://doi.org/10.1038/s41558-019-0630-6
[34] FU X. Land use function change and its driving force of the "production-living-ecological" space in Fenhe River Basin from 1980 to 2020. Chinese Journal of Applied Ecology, 2023, 34(07): 1901-1911. https://doi.org/10.13287/j.1001-9332.202307.022
[35] NURROHMAN R K, KATO T, NINOMIYA H, et al. Future projections of Siberian wildfire and aerosol emissions. Biogeosciences, 2024, 21(18): 4195-4227.https://doi.org/10.5194/bg-21-4195-2024
[36] POTTER C, PASS S, ULRICH R. Net Primary Production of Ecoregions Across North America in Response to Drought and Wildfires From 2015 to 2022. Journal of Geophysical Research-Biogeosciences, 2024, 129(4): e2023JG007750.https://doi.org/10.1029/2023jg007750
[37] WILLEY P. Demographic Vulnerabilities and Wildfire Fatalities. Boca Raton: CRC Press, 2023.
[38] WAGNER C E V. Structure of the Canadian Forest Fire Weather Index: Environment Canada, Canadian Forestry Service, Petawawa Forest Experiment Station, Chalk River, Ontario., 1974.
[39] LIANG L, CHEN M, LUO X, et al. Changes pattern in the population and economic gravity centers since the Reform and Opening up in China: The widening gaps between the South and North. Journal of Cleaner Production, 2021, 310: 127379.https://doi.org/10.1016/j.jclepro.2021.127379
[40] SENANDE-RIVERA M, INSUA-COSTA D, MIGUEZ-MACHO G. Spatial and temporal expansion of global wildland fire activity in response to climate change. Nature Communications, 2022, 13(1): 1208.https://doi.org/10.1038/s41467-022-28835-2
[41] GONG D, YAN C, GUO Z. Vegetation Regeneration After Grassland Fire Based on Remote Sensing Index. Journal of Northwest Forestry University, 2021, 36(06): 204-210.https://doi.org/10.3969/j.issn.1001-7461.2021.06.29